

# ContourCraft: Learning to Resolve Intersections in Neural Multi-Garment Simulations

Artur Grigorev

ETH Zurich  
Switzerland

Max Planck Institute for Intelligent  
Systems  
Germany  
agrigorev@ethz.ch

Giorgio Becherini

Max Planck Institute for Intelligent  
Systems  
Germany

giorgio.becherini@tuebingen.mpg.de

Michael J. Black

Max Planck Institute for Intelligent  
Systems  
Germany

black@tuebingen.mpg.de

Otmar Hilliges

ETH Zurich  
Switzerland

otmar.hilliges@inf.ethz.ch

Bernhard Thomaszewski

ETH Zurich  
Switzerland

bthomasz@ethz.ch

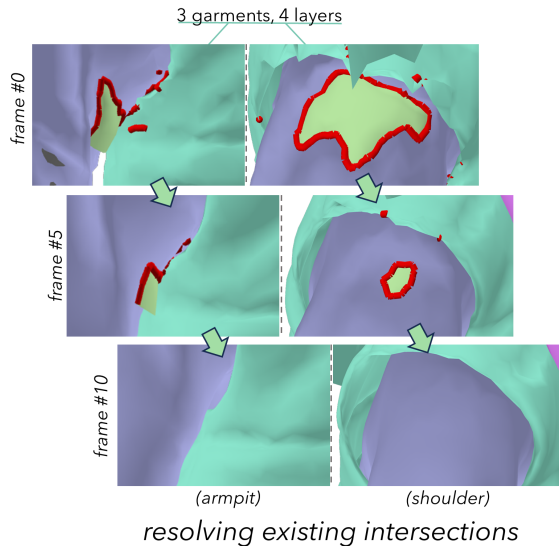


**Figure 1:** We present a novel graph neural network-based approach to learned simulation of multilayered garments. Its key component is an Intersection Contour objective term that encourages resolution of existing cloth–cloth intersections. Even when initialized with intersecting meshes, our approach resolves penetrations (*left*), thus opening the door to learning-based simulation of detailed multi-layer garments (*middle*) and multi-garment outfits (*right*).

## ABSTRACT

Learning-based approaches to cloth simulation have started to show their potential in recent years. However, handling collisions and

intersections in neural simulations remains a largely unsolved problem. In this work, we present ContourCraft, a learning-based solution for handling intersections in neural cloth simulations. Unlike conventional approaches that critically rely on intersection-free inputs, ContourCraft robustly recovers from intersections introduced through missed collisions, self-penetrating bodies, or errors in manually designed multi-layer outfits. The technical core of ContourCraft is a novel intersection contour loss that penalizes interpenetrations and encourages rapid resolution thereof. We integrate our intersection loss with a collision-avoiding repulsion objective into a neural cloth simulation method based on graph neural networks (GNNs). We demonstrate our method’s ability across

Permission to make digital or hard copies of part or all of this work for personal or classroom use is granted without fee provided that copies are not made or distributed for profit or commercial advantage and that copies bear this notice and the full citation on the first page. Copyrights for third-party components of this work must be honored. For all other uses, contact the owner/author(s).  
SIGGRAPH Conference Papers '24, July 27-August 1, 2024, Denver, CO, USA  
© 2024 Copyright held by the owner/author(s).  
ACM ISBN 979-8-4007-0525-0/24/07.  
<https://doi.org/10.1145/3641519.3657408>

a challenging set of diverse multi-layer outfits under dynamic human motions. Our extensive analysis indicates that ContourCraft significantly improves collision handling for learned simulation and produces visually compelling results.

## CCS CONCEPTS

• **Computing methodologies** → **Neural networks; Physical simulation.**

## KEYWORDS

Cloth simulation, garment simulation, collision handling, graph neural networks

### ACM Reference Format:

Artur Grigorev, Giorgio Becherini, Michael J. Black, Otmar Hilliges, and Bernhard Thomaszewski. 2024. ContourCraft: Learning to Resolve Intersections in Neural Multi-Garment Simulations. In *Special Interest Group on Computer Graphics and Interactive Techniques Conference Conference Papers '24 (SIGGRAPH Conference Papers '24)*, July 27-August 1, 2024, Denver, CO, USA. ACM, New York, NY, USA, 11 pages. <https://doi.org/10.1145/3641519.3657408>

## 1 INTRODUCTION

Garment simulation plays a crucial role in video games, animated movies, special effects, fashion design, and many other applications involving digital humans. While conventional methods produce compelling results for complex garments, computational demands for high-quality animations can be significant. Neural simulation methods have emerged as a promising alternative, but a common limitation is their inability to reliably prevent or handle garment intersections. As a result, complex garments and multilayer outfits can exhibit a substantial number of missed intersections, leading to visually disturbing artifacts and overall implausible motion.

Conventional methods, in contrast, aim to maintain intersection-free garments throughout the simulation. With this condition met in the initial state, these methods iteratively resolve all penetrations occurring from one time step to the next. This strategy's critical disadvantage is that it relies on an intersection-free state. Collision response will try to maintain any missed or pre-existing collision, which can compromise entire animation sequences. Unfortunately, intersections due to garment pre-positioning, user interaction, or self-intersecting body motion cannot always be avoided.

In this work, we propose a novel approach for handling intersections in neural cloth simulations (see Fig. 1). Instead of *avoiding* intersections at all costs, we propose a mechanism for *recovering* from existing intersections. We draw inspiration from previous work by Volino and Magnenat-Thalmann [2006], who propose Intersection Contour Minimization (ICM) as a means of resolving penetrations. As our key contribution, we introduce a variational formulation of ICM that allows for direct integration into learning-based methods. The contour loss works in combination with a repulsion term to *avoid and resolve* cloth intersections. We furthermore use intersection contours to identify penetrating regions, which allows us to apply targeted repulsion forces without preventing intersections from resolving. We integrate our new strategy with an existing neural simulation method based on GNNs and unsupervised training [Grigorev et al. 2023].

We demonstrate the effectiveness of our method by simulating a diverse set of complex multi-layer outfits for dynamic human motion. In particular, we show that our method rapidly recovers from heavily intersecting configurations of complex multi-layer outfits. Intersections introduced during fast or self-penetrating motion of the underlying body are also reliably resolved. All results can be reproduced using our publicly available source code<sup>1</sup>.

## 2 RELATED WORK

Most related to our work is research on collision handling for garment simulation and learning-based approaches to cloth simulation.

*Collision Handling for Garment Simulation.* Detecting and handling collisions has been a central focus of computer animation for several decades [Baraff et al. 2003; Teschner et al. 2005]. Bridson et al. [2002] presented a three-tier collision-handling pipeline that uses impulses, i.e., velocity corrections, to prevent imminent collisions. The first stage applies repelling impulses that push primitives apart that are too close together. The second stage uses continuous collision detection (CCD) and corresponding impulses to resolve intersections occurring during time steps. Any collisions that remain after the second stage are treated using rigid impact zones, which cancel relative velocities between regions spanning multiple collision primitives. This impulse-based collision handling framework has been widely adopted and extended in various ways [Harmon et al. 2008].

Whereas the approach by Bridson et al. [2002] decouples time integration and collision handling, recent work explores more closely coupled treatments. Harmon et al. [2009] describe an approach for asynchronous time stepping of contact dynamics that guarantees robustness at the expense of significantly increased computation times. More recently, IPC [Li et al. 2020] provides robust and fully implicit treatment of contact dynamics using smoothly clamped log barrier functions. While IPC can generate compelling animations with complex and challenging self-collisions, computation times are on the order of minutes per frame.

Another line of work [Tang et al. 2018a, 2011, 2013, 2018b; Wang 2021; Wang et al. 2017; Wu et al. 2020] aims to accelerate the collision handling process by developing efficient and highly parallelizable algorithms that leverage the processing power of GPUs. These works mainly focus on optimizing the CCD step as it is the most time-consuming part of the collision handling process. The modifications to CCD include efficient hashing to accelerate the traversal of bounding volume hierarchies (BVH) [Karras 2012; Tang et al. 2018a], tests that enable parts of the BVH to be skipped [Wang et al. 2017], and incremental collision detection that handles only triangles affected by collision-response steps [Wang et al. 2017]. While being much faster than non-optimized CPU algorithms, these approaches still perform the same sequence of steps used in the classical method of [Bridson et al. 2002]. Wu et al. [2020] and Wang [2021] propose to substitute continuous collision constraints with a set of discrete ones that greatly improve the simulation speed. However, to do that they rely on a regular grid-like mesh structure maintained by dynamic re-meshing.

<sup>1</sup>URL will be disclosed upon acceptance.

All of the above methods require intersection-free geometry as input and follow the conventional strategy of detecting and resolving new collisions between time frames. Because of that, they struggle to recover from intersections that either exist in the initial geometry or occur during the simulation. The same mechanisms that prevent intersections from occurring also prevent them from being resolved.

Few works have tackled the problem of resolving existing intersections. Baraff et al. [2003] detect connected components separated from the rest of the mesh by a closed contour of penetrations. To resolve these intersections, their method applies attractive forces to the pairs of such components. While intersections with closed contours can be resolved in this way, their method does not address open-contour intersections such as penetrating pairs of mesh boundaries. Intersection Contour Minimization (ICM) [Volino and Magnenat-Thalmann 2006] aims to resolve cloth intersections in the general case by minimizing the length of intersection contours. For each pair of intersecting triangles, ICM computes the gradient of intersection length with respect to the mesh vertices involved in the corresponding collisions. It then iteratively applies local displacements in the negative direction of the gradients such as to resolve the intersections. While several subsequent works have adopted and extended this idea [Cha and Ko 2020; Ye et al. 2017, 2015; Ye and Zhao 2012; Zhong 2009], we are the first to explore Intersection Contour Minimization in the context of learned garment simulation. Rather than applying intersection-resolving forces, we train a GNN with an objective term that penalizes the total length of the intersections. In this way, our model learns to resolve intersections in an unsupervised manner.

*Learning-Based Cloth Simulation.* To avoid the high computational cost of physics-based cloth simulation, a recent stream of work has started to explore learning-based techniques for this task. Learned deformation models are commonly used to model garment behavior [Bertiche et al. 2022; Guan et al. 2012; Santesteban et al. 2019, 2022a, 2021]. These models predict garment deformations based on the pose and shape of the underlying body model. While offering fast inference due to their relatively small network sizes, they have to be retrained separately for each garment and cannot generalize to unseen ones. As an alternative approach, MeshGraphNets [Pfaff et al. 2021] uses graph neural networks to learn mesh-based simulations from examples. Trained on cloth simulation data, MeshGraphNets learns to handle cloth–cloth interactions in the process. Taking this approach one step further, HOOD [Grigorev et al. 2023] learns the dynamic behavior of garments and their interaction with the human body. The unsupervised physics-guided training, inspired by PBNS [Bertiche et al. 2020] and SNUG [Santesteban et al. 2022a], alleviates the need for curated simulation data. However, HOOD is unable to model cloth–cloth interactions and self-collisions, leading to unrealistic results for multi-layer outfits. LayersNet [Shao et al. 2023] employs a transformer-based approach to model multi-layer outfits. However, it requires a large dataset of physically simulated ground-truth data to train.

Several recent learning-based approaches proposed strategies to address garment collisions. For instance, Repulsive Force Unit (ReFU) [Tan et al. 2022] operates as a plug-in layer that processes the human body as a signed distance field (SDF), pushing garment

nodes and edges outside of it. Implicit Untangling [Buffet et al. 2019] and ULNeF [Santesteban et al. 2022b] both use implicit representations for garment untangling. Given a set of interpenetrating garments in a canonical pose, these techniques resolve penetrations by arranging garments in a specific order, i.e., from innermost to outermost. However, these methods only consider static garments in a single canonical pose and do not handle dynamic collisions. PBNS [Bertiche et al. 2020] prevents inter-garment penetrations in various poses by applying a collision penalty between layer-ordered garments during training. For each garment, PBNS finds and penalizes intersections with the body and lower-level garments. However, PBNS requires training a separate model for each set of garments and does not account for intra-garment collisions, making it unsuitable for modeling multi-layer outfits. In summary, while some learning-based methods account for penetrations between different garments, none of them addresses the problem of preventing and resolving garment self-penetrations in dynamic scenes. Our approach addresses this significantly more challenging problem by training a GNN to prevent and resolve garment intersections.

Another recent stream of work investigates using neural networks to learn nonlinear subspaces for rapid simulation [Fulton et al. 2019; Holden et al. 2019; Sharp et al. 2023; Shen et al. 2021; Wang et al. 2024]. A notable example in this context is the method by Romero et al. [2021] that learns contact corrections for handle-based subspace dynamics. While these methods can yield substantial accelerations compared to full space simulation, the networks are trained for a given input mesh and do not generalize to new input geometry.

### 3 BACKGROUND: LEARNED GARMENT SIMULATION

MeshGraphNets [Pfaff et al. 2021] approaches the task of cloth simulation with the help of graph-based neural networks. HOOD [Grigorev et al. 2023] takes this approach one step further and demonstrates how such a model can be trained in an unsupervised physics-guided fashion to predict the dynamics of garments and their interactions with the human body. HOOD takes as input a graph containing nodes  $V^G$  and edges  $E^G$  of the garment mesh augmented with so-called *body edges*,  $E^B$ , that connect the garment vertices to the nodes of the body mesh  $V^B$ . Each node and edge of the input mesh is endowed with a corresponding feature vector that describes properties such as nodal mass, velocity, and rest length of the mesh edge. The feature vectors are then mapped into latent space, updated through several message-passing steps, and finally decoded into nodal accelerations. The complete process can be written as

$$\hat{A} = f_{\theta}(V^G, V^B, E^G, E^B), \quad (1)$$

where  $\hat{A}$  are the predicted accelerations for each garment node and  $f_{\theta}$  is the GNN.

The network is trained in an unsupervised manner with the objective function consisting of a set of energies produced by stretching, bending, inertia, and other physical phenomena,

$$\mathcal{L}_{\text{HOOD}} = \mathcal{L}_{\text{bending}} + \mathcal{L}_{\text{stretching}} + \mathcal{L}_{\text{gravity}} + \quad (2)$$

$$+ \mathcal{L}_{\text{friction}} + \mathcal{L}_{\text{collision}}^{\text{body}} + \mathcal{L}_{\text{inertia}}. \quad (3)$$

Building on an optimization-based variant of implicit Euler integration [Martin et al. 2011], the model is thus encouraged to predict accelerations that balance kinetic and potential energy in a robust and physically plausible way. This method’s main drawback is that it completely ignores cloth–cloth interactions, rendering it unsuitable for modeling detailed multi-layer garments and multi-garment outfits. We address this limitation by extending HOOD with an intersection contour loss term and supplying it with information about cloth interactions.

## 4 METHOD

Our method builds on the concept of intersection contours [Volino and Magnenat-Thalmann 2006]. We first use intersection contours to differentiate between repulsive and non-repulsive cloth–cloth interactions. Then, we define intersection contour length as an additional loss term to encourage the model to resolve existing intersections.

To evaluate the advantages of our method, we conduct a detailed ablation study in which we progressively modify the GNN-based approach by Grigorev et al. [2023]. In this section, we describe and explain the motivation behind each modification.

### 4.1 Conventional Collision Handling with GNNs

To establish a meaningful baseline, we first develop a direct implementation of conventional collision handling for GNNs. To this end, we augment the GNN model with correspondences between spatially close pieces of cloth and include a new repulsion term into its loss function. This enables the GNN to prevent the majority of penetrations.

**4.1.1 Cloth–Cloth Correspondences.** Following MeshGraphNets [Pfaff et al. 2021], we expand the input graph to incorporate cloth–cloth correspondences. To identify these correspondences, we detect all face–node pairs for which (a) the projection of the node along the face normals falls inside the face and (b) the corresponding distance is smaller than a given threshold  $\epsilon$  (see Algorithm 1). Condition (a) limits the number of correspondences in the graph and thus accelerates inference. For each such pair, we add a “world edge” to the graph connecting the node to the closest triangle vertex from the pair.

The forward pass of the model is formulated as

$$\hat{A} = f_{\theta}(V^G, V^B, E^G, E^B, E^W), \quad (4)$$

where  $E^W$  is a set of world edges.

**4.1.2 Repulsion Loss.** To make use of the cloth–cloth correspondences, we augment the training objective with a new repulsion term,

$$\mathcal{L}_{repulsion} = \sum_i \max(\xi - d_{curr}^{(i)} \cdot \text{sign}(d_{prev}^{(i)}), 0)^3, \quad (5)$$

where  $d_{curr}^{(i)}$  and  $d_{prev}^{(i)}$  are distances between the node  $v^{(i)}$  and the corresponding face  $f^{(i)}$  in the current and previous frames respectively,

$$d^{(i)} = ((v^{(i)} - f^{(i)}) \cdot \vec{n}^{(i)}). \quad (6)$$

The repulsion term penalizes face–node pairs in which the node either crosses the face or comes closer to it than a given repulsion threshold  $\xi$ , corresponding to the fabric’s thickness (we use  $\xi = 1mm$ ).

Since in this version, all cloth interactions are penalized by the repulsive loss, we refer to it as “only repulsive”. Its full objective term is

$$\mathcal{L}_{repulsive}^{\text{only}} = \mathcal{L}_{HOOD} + \mathcal{L}_{repulsion}. \quad (7)$$

These two modifications enable the model to prevent most penetrations, but they do come with two major drawbacks. First, the updated model can still miss collisions. Therefore, a fail-safe method based on conventional, non-learned collision handling is still required for realistic simulations. Second, such a method would still struggle to recover from existing penetrations—the mechanisms designed to prevent self-intersections from occurring also prevent their resolution.

### 4.2 Repulsive and non-repulsive interactions

To resolve existing self-intersections we must distinguish between two types of cloth–cloth interactions. In an intersection-free state, spatially close regions of cloth need to be repelled from each other. However, for existing intersections, such a response might prevent them from being resolved.

We distinguish between repulsive and non-repulsive interactions in the following way. First, we run discrete collision detection (DCD) to determine all penetrating triangle pairs. We then combine sequences of adjacent penetrations into intersection contours. Each contour may be either open or closed. The latter splits the surface into two disconnected parts. In this case, we consider the smaller part to lie inside the contour, and the larger one to lie outside. To handle cases with nested closed contours, we only keep the outermost ones. Finally, we mark as “non-repulsive” the interactions where at least one node is either (a) part of an open contour or (b) lies inside a closed contour. See Fig. 2 for illustration.

The distinction between repulsive and non-repulsive interactions translates into the corresponding world edges in the input graph. This leads to an updated expression for nodal accelerations,

$$\hat{A} = f_{\theta}(V^G, V^B, E^G, E^B, E_R^W, E_{NR}^W), \quad (8)$$

where  $E_R^W$  and  $E_{NR}^W$  are world edges corresponding to repulsive and non-repulsive interactions, respectively.

### 4.3 Naïve baseline

The simplest way of dealing with intersections is to ignore them. That is, to ignore those cloth–cloth interactions that participate in any penetration. We implement this strategy as an ablated model (“w/o IC loss”) where all such correspondences are omitted from the graph. In this way, the model does not prevent existing intersections from being resolved but does not try to purposefully recover from them.

### 4.4 Intersection Contour Loss

To train the model to resolve cloth intersections we employ a simple but effective objective term that we refer to as *Intersection Contour Loss* ( $\mathcal{L}_{IC}$ ). This term is based on the lengths of all triangle–triangle intersections. Here we describe the process of computing this term in detail.

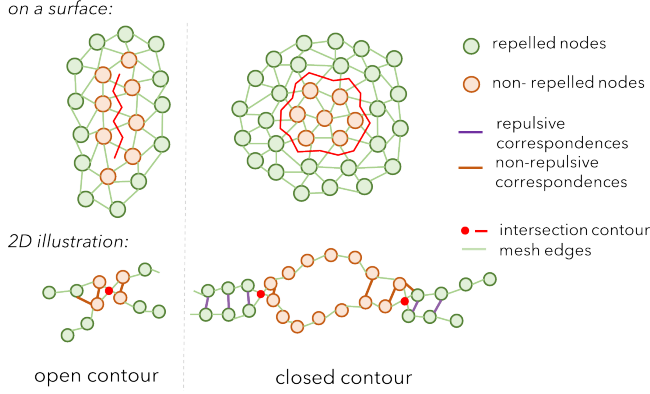


**Figure 2:** We distinguish between two types of garment nodes. Repelled nodes are those that either do not participate in the penetrations or lie outside a closed contour. Non-repelled nodes are those that are either part of an open contour or lie inside a closed one. If a triangle-node correspondence only contains repulsive nodes, we define this correspondence as repulsive and apply a repulsion loss to it, otherwise it is non-repulsive.

Each triangle–triangle intersection detected by DCD contains two edge–triangle intersections. For each of them, we can first find the relative coordinate  $s$  of the intersection point on the edge,

$$s = \frac{(x_\Delta \cdot \vec{n}) - (x_0 \cdot \vec{n})}{(x_1 - x_0) \cdot \vec{n}}, \quad (9)$$

where  $x_0$  and  $x_1$  are vertices of the intersecting edge,  $x_\Delta$  is a point inside the triangle, and  $\vec{n}$  is the triangle’s normal vector. The coordinates of the intersection point are computed as

$$p_{I_i^j} = dg(x_0) + s \cdot dg(x_1 - x_0), \quad (10)$$

where  $i$  is the index of the intersecting triangle pair and  $j$  is the index of the edge–triangle intersection within it. The function  $dg()$  indicates that we do not use the partial derivative of this term w.r.t. its arguments when computing the gradient during training (see Section 4.5 for details). Finally, the loss term is computed as a sum of the squared lengths of all intersections,

$$\mathcal{L}_{IC} = \sum_i \|p_{I_i^0} - p_{I_i^1}\|^2. \quad (11)$$

The full objective function is thus

$$\mathcal{L}_{ours} = \mathcal{L}_{HOOD} + \lambda_1 \mathcal{L}_{repulsion} + \lambda_2 \mathcal{L}_{IC}, \quad (12)$$

where  $\lambda_1$  and  $\lambda_2$  are weighting coefficients. In this setting, the repulsive correspondences are explicitly penalized by the repulsion loss, while non-repulsive ones are penalized implicitly by the Intersection Contour Loss.

#### 4.5 Intersection Contour Gradient

While the intersection contour objective is straightforward to integrate with the physics-based loss, directly using it during training leads to sub-optimal results. Fig. 3 shows an example in which the gradient of length for a single contour segment is decomposed into its partial derivatives. One of the components reduces length by distorting the triangle, whereas the other one achieves length

reduction through translational motion. Please refer to the Supplemental Material for details. While nominally reducing length, we empirically observe that the distortional component is generally not helpful for resolving intersections as it induces compression in the fabric and provokes strong reaction forces. For this reason, we use only the partial gradient corresponding to quasi-rigid translation during training. This strategy successfully reduces distortion artifacts and, as our statistical analysis shows (Table 1, Fig. 5), leads to fewer intersections overall. In our experiments we refer to the model where both components are used as “full gradient.”

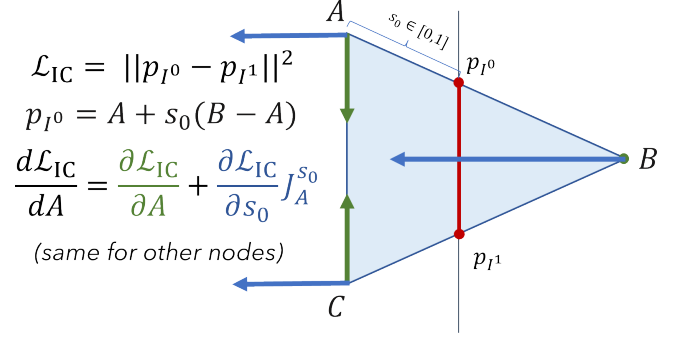


**Figure 3:** A face (blue triangle) intersects a perpendicular plane (vertical line with intersecting segment shown in red). Green arrows show the negative partial gradients of the contour loss  $\mathcal{L}_{IC}$  w.r.t. the triangle nodes. Blue arrows indicate negative partial gradients w.r.t. the coordinate of the intersection point  $s_j$ . The former gradient (green) squeezes the triangle to decrease the contour length, while the latter (blue) moves it along the plane’s normal direction to resolve the intersection. We only use the gradient w.r.t.  $s_j$  in our training.  $J_A^{s_0}$  is the Jacobian of  $s_0$  w.r.t.  $A$ .

---

#### ALGORITHM 1: *findClothCorrespondences*

---

**Input:** Outfit mesh with vertices  $V$  and faces  $F$   
 correspondences  $\leftarrow \{\emptyset\}$   
**foreach**  $v \in V$  **do**  
   **foreach**  $f \in F$  **do**  
     **if**  $v \in f$  **then**  
       | **continue**  
     **if** distance( $v, f$ )  $> \epsilon$  **then**  
       | **continue**  
      $v_{proj} \leftarrow$  projection of  $v$  onto  $f$   
     **if**  $v_{proj}$  inside  $f$  **then**  
       | correspondences.append( $(v, f)$ )  
**return** correspondences

---

#### 4.6 Building the input graph

Algorithm 2 shows the overall process of building the input graph for the GNN. Similar to HOOD, we initialize from a graph of the mesh edges (*buildGraph*) and then augment them with edges to the closest body nodes (*addBodyEdges*). We then detect intersecting triangle pairs within the outfits with DCD and combine adjacent intersections into intersection contours (*makeContours*), removing contours that are enclosed by others (*removeNested*). Finally, we

**ALGORITHM 2: *buildInputGraph***


---

```

Input: Outfit mesh with vertices  $V_g$  and faces  $F_g$ 
Input: Body mesh with vertices  $V_b$  and faces  $F_b$ 
 $G \leftarrow \text{buildGraph}(V_g, F_g)$  // build graph from mesh edges
 $G \leftarrow \text{addBodyEdges}(G, V_b)$  // add "body edges" as in HOOD
penetrations  $\leftarrow \text{DCD}(V_g, F_g)$ 
contours  $\leftarrow \text{makeContours}(\text{penetrations})$ 
contours  $\leftarrow \text{removeNested}(\text{contours})$ 
clothCorrespondences  $\leftarrow \text{findClothCorrespondences}(V_g, F_g)$ 
foreach  $C \in \text{clothCorrespondences}$  do
  isRepulsive  $\leftarrow \text{True}$ 
  foreach  $v \in C$  do comment
    foreach contour  $\in \text{contours}$  do
      if  $v$  is part of or enclosed within contour then
        if isClosed(contour) then
          if  $v$  inside contour then
            isRepulsive  $\leftarrow \text{False}$ 
          else
            isRepulsive  $\leftarrow \text{False}$ 
         $G \leftarrow \text{addWorldEdge}(G, C, \text{isRepulsive})$ 
  return  $G$ 

```

---

find face–node correspondences in world coordinates (*findClothCorrespondences*, Algorithm 1), classify them into repulsive and non-repulsive, and add corresponding world edges to the graph.

#### 4.7 Training process

Our method is trained to autoregressively predict nodal accelerations that generate realistic garment motions and also prevent and resolve cloth self-intersections. We split the training process into three stages.

The first stage follows exactly the training process of HOOD [Grigorev et al. 2023]. Its goal is to train a model to realistically mimic the physical behavior while ignoring cloth–cloth interactions. To this end, we exclude the corresponding interactions from the input graph and train it with the original objective function,  $\mathcal{L}_{\text{HOOD}}$ .

The second stage aims to teach the model to *prevent* cloth self-intersections. For this purpose, we remove all self-intersections from the garment mesh in the initial frame and then resolve all collisions happening between frames using the method by Bridson et al. [2002]. If the algorithm fails to resolve all collisions in a given number of iterations, we stop the simulation of the current sequence and move on to the next one in the dataset. Note that the algorithm by Bridson et al. [2002] is only used to maintain intersection-free geometry in this stage of the training process and is not part of the loss function. In this stage, all cloth–cloth interactions are treated as *repulsive*, so the objective function is  $\mathcal{L}_{\text{HOOD}} + \mathcal{L}_{\text{repulsion}}$ .

The third stage is designed to teach the model to *resolve* cloth intersections. Here, we again initialize from potentially self-intersecting geometry without resorting to [Bridson et al. 2002] and classify the cloth–cloth interactions into *repulsive* and *non-repulsive* ones (see Fig. 2). During this stage, we use the full objective function,  $\mathcal{L}_{\text{HOOD}} + \mathcal{L}_{\text{repulsion}} + \mathcal{L}_{\text{IC}}$ . For more details on implementation and the training process, please refer to the supplemental material.

## 5 RESULTS

### 5.1 Pose sequences and garment meshes

Our method is trained in an unsupervised physically guided fashion without the need for ground-truth physical simulations. The only data necessary for training and inference are human body pose sequences and static outfit meshes.

For training we use the same pose sequences from AMASS [Mahmood et al. 2019] that were used in Grigorev et al. [2023]; Santesteban et al. [2022a, 2021]. We train the model using a combination of simple one-layer garments used in Grigorev et al. [2023]; Santesteban et al. [2022a] and three multi-layer outfits from the BEDLAM dataset [Black et al. 2023].

For our experiments, we use the same eight pose sequences from AMASS as Grigorev et al. [2023] and model five multi-layer outfits from BEDLAM: two outfits with two garments, two outfits with three garments, and one with five garments. Please see the supplementary material for more details. These outfits were not seen by the model during training. In total this amounts to 40 validation sequences. We start the simulations from the first frame of the pose sequence without initialization steps that interpolate between the T-pose and the first frame pose. To initialize the garment geometry, we use simple linear blend skinning with the skinning weights collected from the body model. This means the initial garment geometries may have severe self-penetrations, which our method can resolve (see Fig. 1, left).

To illustrate the practicality of our method, we show rendered sequences of our clothing simulations using the Unreal engine. Please refer to the supplementary video for more results.

### 5.2 Ablation study

We compare our method to three ablated models introduced in Section 4. To reiterate, in *"only repulsive"* we consider all cloth–cloth interactions as repulsive; in *"w/o IC loss"* we distinguish between repulsive and non-repulsive interactions, but do not apply any supervision to the non-repulsive ones; in *"full gradient"* we use the Intersection Contour loss with full gradient (see Fig. 3).

We simulate all 40 validation sequences with each of the ablated models and compare their performance in terms of the average number of intersecting triangle pairs in each frame. Table 1 shows that each modification we introduce significantly reduces the number of intersections in simulated sequences.

Fig. 5 shows how well each ablated model resolves the intersections in the initial geometry. For each frame, it plots the fraction of the remaining intersections relative to the initial geometry. This information is aggregated across all 40 validation sequences. Fig. 6 plots the number of intersections for each frame of a single sequence. Both of these plots demonstrate the improvements in collision handling by each modification.

### 5.3 Perceptual study

Additionally, we perform a perceptual study to assess the realism of ContourCraft results as perceived by human subjects. We compare ContourCraft to CLO3D [CLO Virtual Fashion 2022], a commercial software for garment design and modeling, and two baseline methods: HOOD [2023] and linear blend skinning (LBS)

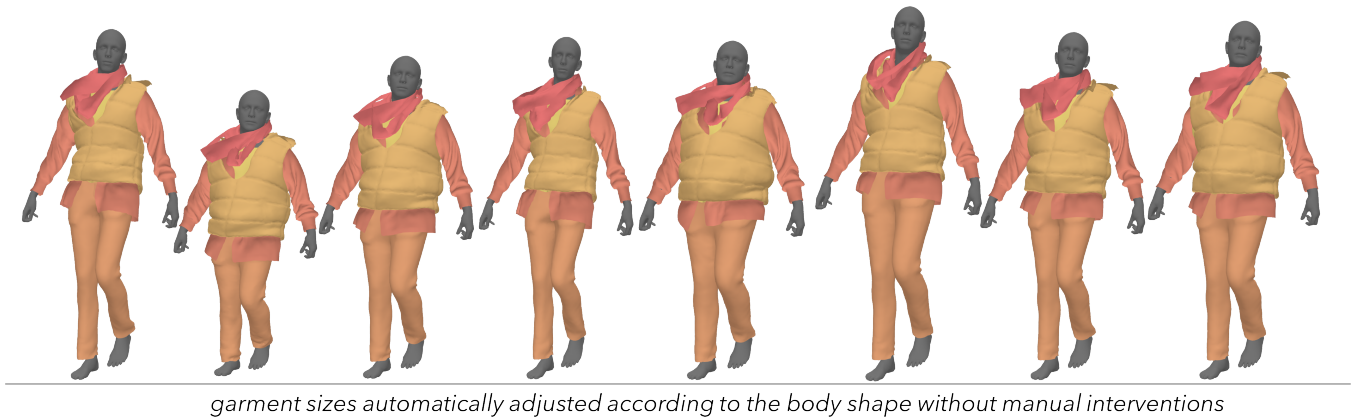


**Figure 4:** Since our method can resolve intersections present in the initial geometry, we can model automatically resized outfits without manual resolution of the intersections arising during this process.

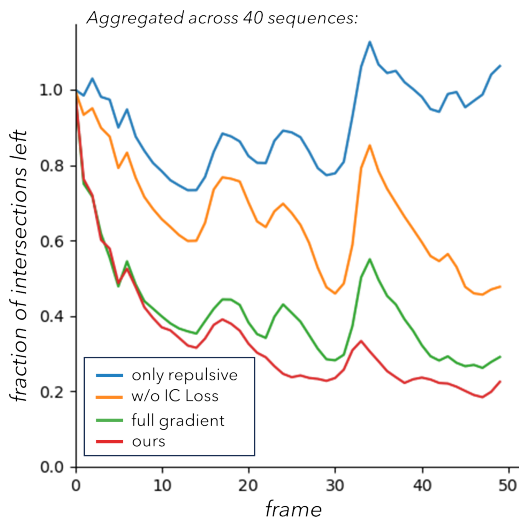


**Figure 5:** The plot shows the fraction of the triangle-triangle intersections left after each frame (up to 50) relative to the initial geometry. The values are aggregated across the whole validation set (40 sequences). Note that during dynamic movements new intersections may appear, hence the plot is not monotonic.

**Table 1:** We compare our method to three ablated versions in terms of an average number of penetrating triangle pairs. Each additional term provides substantial improvements to collision handling.

	2 garments avg. 13016 nodes	3 garments avg. 18981 nodes	5 garments 36515 nodes	all outfits avg. 20102 nodes
HOOD	1347	5673	38480	8796
only repulsive	373.2	1069	25220	4424
w/o IC loss	122.2	268.4	1491	391
full gradient	74.9	163.4	1315	299
ours	<b>55.9</b>	<b>126.6</b>	<b>481.2</b>	<b>150</b>

The study consists of two parts. In the first part, the participants were asked to rate the realism of the simulations on a scale from 1 to 5. CLO3D scored on average **4.29**, ContourCraft scored **4.15**, LBS achieved **3.04**, and HOOD was rated **2.78**. In the second part, the two baselines and ContourCraft were compared to CLO3D. The participants were asked to choose which of the two simulations (shown side-by-side) was more realistic. Here, LBS was preferred over CLO3D in **16.5%** of the cases, HOOD in **16.9%** of the cases, and ContourCraft in **35.8%** of the cases.

These results demonstrate that, although ContourCraft cannot achieve the level of realism of commercial software such as CLO3D, its results are not much inferior in terms of perceived realism. For more details on the study please refer to the supplemental material.

#### 5.4 Automatic outfit resizing

When designing 3D outfits, it is highly desirable to automatically adjust the size of the garments to the body shape. However, in the case of multi-layer outfits, automatically resizing them may introduce unwanted cloth intersections. To simulate such outfits, these penetrations have to be manually resolved by an artist because the simulation software may struggle to recover from them.

Since our method is trained to resolve existing intersections, it can handle penetrations caused by automatic resizing. We demonstrate this in Fig. 4 and in the supplemental video. Here, we use a single original outfit geometry that fits the canonical SMPL-X [Pavlakos et al. 2019] template body and then resize it to a new body shape by randomly sampling body shape parameters from a normal distribution with  $\sigma = 3$ . To resize the outfits, for each garment node, we sample shape blend shapes from the SMPL-X vertex closest to it. We then modify the nodal positions using the same shape vectors as for the body. Our method robustly recovers from the intersections that arise during this process, allowing it to realistically model the resized outfits.

## 6 CONCLUSION

ContourCraft is a novel method for modeling complex multi-layer outfits in motion. Its core is a new Intersection Contour Loss term that allows the GNN-based model to resolve cloth intersections

that are present in the initial geometry or occur during simulation. At the same time, our model can prevent most of the penetrations from happening in the first place, ensuring realistic simulation. In addition to the detailed quantitative analysis of our contributions, we show how to easily resize complex outfits to new body sizes while resolving interpenetrations. With the field of learned physical simulation of garments still in its infancy, we show that the flexibility of learned models holds promise for problems that are traditionally difficult for conventional physics-based simulation, including the resolution of existing self-intersections.

## 7 LIMITATIONS AND FUTURE WORK

Despite the overall efficiency of our learned method for handling cloth intersections, there are cases that are difficult to resolve due to the nature of the Intersection Contour loss. For example, in dynamic sequences, small non-manifold pieces of cloth (e.g. pockets) may pop outside the garment in a single frame. In those cases, the model will assume that this is the correct configuration since trying to pull the pocket back inside would increase the length of the contour. Similarly, if initialized with geometry in which two garments are entangled in a way where it is impossible to infer their correct order, our method will also fail.

While we base our method on a learned physical simulator [Grigorev et al. 2023], one direction for future work is applying the formulation of Intersection Contour Loss to pose-driven garment deformation models such as PBNS [Bertiche et al. 2020] and SNUG [Sansteban et al. 2022a] that offer faster inference compared to HOOD.

## ACKNOWLEDGMENTS

AG was supported in part by the Max Planck ETH Center for Learning Systems. We thank Joachim Tesch, Christoph Gebhardt, Xu Chen, and Peter Kulits for their feedback and help during the project.

## REFERENCES

- David Baraff, Andrew Witkin, and Michael Kass. 2003. Untangling cloth. *ACM Transactions on Graphics (TOG)* 22, 3 (2003), 862–870.
- Hugo Bertiche, Meysam Madadi, and Sergio Escalera. 2020. PBNS: physically based neural simulator for unsupervised garment pose space deformation. *arXiv preprint arXiv:2012.11310* (2020).
- Hugo Bertiche, Meysam Madadi, and Sergio Escalera. 2022. Neural Cloth Simulation. *ACM Transactions on Graphics (TOG)* 41, 6 (2022), 1–14.
- Michael J. Black, Priyanka Patel, Joachim Tesch, and Jinlong Yang. 2023. BEDLAM: A Synthetic Dataset of Bodies Exhibiting Detailed Lifelike Animated Motion. In *Proceedings IEEE/CVF Conf. on Computer Vision and Pattern Recognition (CVPR)*.
- Robert Bridson, Ronald Fedkiw, and John Anderson. 2002. Robust treatment of collisions, contact and friction for cloth animation. In *Proceedings of the 29th annual conference on Computer graphics and interactive techniques*. 594–603.
- Thomas Buffet, Damien Rohmer, Loic Barthe, Laurence Boissieux, and Marie-Paule Cani. 2019. Implicit untangling: A robust solution for modeling layered clothing. *ACM Transactions on Graphics (TOG)* 38, 4 (2019), 1–12.
- Ick-Hoon Cha and Hyeon-Seok Ko. 2020. Tanglement resolution in clothing simulation with explicit convergence. *IEEE Transactions on Visualization and Computer Graphics* 28, 7 (2020), 2764–2775.
- CLO Virtual Fashion. 2022. *Clo3D*. CLO Virtual Fashion. <https://clo3d.com/en/Computer Software>.
- Lawson Fulton, Vismay Modi, David Duvenaud, David I. W. Levin, and Alec Jacobson. 2019. Latent-space Dynamics for Reduced Deformable Simulation. *Computer Graphics Forum* (2019).
- Artur Grigorev, Bernhard Thomaszewski, Michael J Black, and Otmar Hilliges. 2023. HOOD: Hierarchical Graphs for Generalized Modelling of Clothing Dynamics. *IEEE/CVF Conf. on Computer Vision and Pattern Recognition (CVPR)*.
- Peng Guan, Loretta Reiss, David A Hirschberg, Alexander Weiss, and Michael J Black. 2012. Drape: Dressing any person. *ACM Transactions on Graphics (ToG)* 31, 4 (2012), 1–10.
- David Harmon, Etienne Vouga, Breannan Smith, Rasmus Tamstorf, and Eitan Grinspun. 2009. Asynchronous contact mechanics. *ACM Transactions on Graphics* 28 (7 2009). Issue 3. <https://doi.org/10.1145/1531326.1531393>
- David Harmon, Etienne Vouga, Rasmus Tamstorf, and Eitan Grinspun. 2008. Robust treatment of simultaneous collisions. In *ACM SIGGRAPH 2008 papers*. 1–4.
- Daniel Holden, Bang Chi Duong, Sayantan Datta, and Derek Nowrouzezahrai. 2019. Subspace Neural Physics: Fast Data-Driven Interactive Simulation. In *Proceedings of the 18th Annual ACM SIGGRAPH/Eurographics Symposium on Computer Animation* (Los Angeles, California) (SCA '19). Association for Computing Machinery, New York, NY, USA, Article 6, 12 pages. <https://doi.org/10.1145/3309486.3340245>
- Tero Karras. 2012. Maximizing parallelism in the construction of BVHs, octrees, and k-d trees. In *Proceedings of the Fourth ACM SIGGRAPH/Eurographics conference on High-Performance Graphics*. 33–37.
- Minchen Li, Zachary Ferguson, Teseo Schneider, Timothy R Langlois, Denis Zorin, Daniele Panozzo, Chenfanfu Jiang, and Danny M Kaufman. 2020. Incremental potential contact: intersection-and inversion-free, large-deformation dynamics. *ACM Trans. Graph.* 39, 4 (2020), 49.
- Naureen Mahmood, Nima Ghorbani, Nikolaus F Troje, Gerard Pons-Moll, and Michael J Black. 2019. AMASS: Archive of motion capture as surface shapes. In *Proceedings of the IEEE/CVF international conference on computer vision*. 5442–5451.
- Sebastian Martin, Bernhard Thomaszewski, Eitan Grinspun, and Markus Gross. 2011. Example-Based Elastic Materials. *ACM Trans. Graph.* 30, 4, Article 72 (jul 2011), 8 pages. <https://doi.org/10.1145/2010324.1964967>
- Georgios Pavlakos, Vasileios Choutas, Nima Ghorbani, Timo Bolkart, Ahmed A. A. Osman, Dimitrios Tzionas, and Michael J. Black. 2019. Expressive Body Capture: 3D Hands, Face, and Body from a Single Image. In *Proceedings IEEE Conf. on Computer Vision and Pattern Recognition (CVPR)*.
- Tobias Pfaff, Meire Fortunato, Alvaro Sanchez-Gonzalez, and Peter W Battaglia. 2020. Learning mesh-based simulation with graph networks. *arXiv preprint arXiv:2010.03409* (2020).
- Tobias Pfaff, Meire Fortunato, Alvaro Sanchez-Gonzalez, and Peter W. Battaglia. 2021. Learning Mesh-Based Simulation with Graph Networks. In *International Conference on Learning Representations*.
- Cristian Romero, Dan Casas, Jesús Pérez, and Miguel Otaduy. 2021. Learning Contact Corrections for Handle-Based Subspace Dynamics. *ACM Trans. Graph.* 40, 4, Article 131 (jul 2021), 12 pages. <https://doi.org/10.1145/3450626.3459875>
- Igor Santesteban, Miguel Otaduy, Nils Thuerey, and Dan Casas. 2022b. Ulnef: Untangled layered neural fields for mix-and-match virtual try-on. *Advances in Neural Information Processing Systems* 35 (2022), 12110–12125.
- Igor Santesteban, Miguel A Otaduy, and Dan Casas. 2019. Learning-based animation of clothing for virtual try-on. In *Computer Graphics Forum*, Vol. 38. Wiley Online Library, 355–366.
- Igor Santesteban, Miguel A Otaduy, and Dan Casas. 2022a. Snug: Self-supervised neural dynamic garments. In *Proceedings of the IEEE/CVF Conference on Computer Vision and Pattern Recognition*. 8140–8150.
- Igor Santesteban, Nils Thuerey, Miguel A Otaduy, and Dan Casas. 2021. Self-supervised collision handling via generative 3d garment models for virtual try-on. In *Proceedings of the IEEE/CVF Conference on Computer Vision and Pattern Recognition*. 11763–11773.
- Yidi Shao, Chen Change Loy, and Bo Dai. 2023. Towards Multi-Layered 3D Garments Animation. *arXiv preprint arXiv:2305.10418* (2023).
- Nicholas Sharp, Cristian Romero, Alec Jacobson, Etienne Vouga, Paul Kry, David I.W. Levin, and Justin Solomon. 2023. Data-Free Learning of Reduced-Order Kinematics. In *ACM SIGGRAPH 2023 Conference Proceedings* (<conf-loc>, <city>Los Angeles</city>, <state>CA</state>, <country>USA</country>, </conf-loc>) (SIGGRAPH '23). Association for Computing Machinery, New York, NY, USA, Article 40, 9 pages. <https://doi.org/10.1145/3588432.3591521>
- Siyuan Shen, Yin Yang, Tianjia Shao, He Wang, Chenfanfu Jiang, Lei Lan, and Kun Zhou. 2021. High-Order Differentiable Autoencoder for Nonlinear Model Reduction. *ACM Trans. Graph.* 40, 4, Article 68 (jul 2021), 15 pages. <https://doi.org/10.1145/3450626.3459754>
- Qingyang Tan, Yi Zhou, Tuanfeng Wang, Duygu Ceylan, Xin Sun, and Dinesh Manocha. 2022. A Repulsive Force Unit for Garment Collision Handling in Neural Networks. In *Computer Vision—ECCV 2022: 17th European Conference, Tel Aviv, Israel, October 23–27, 2022, Proceedings, Part III*. Springer, 451–467.
- Min Tang, Zhongyuan Liu, Ruofeng Tong, and Dinesh Manocha. 2018a. PSCC: Parallel self-collision culling with spatial hashing on GPUs. *Proceedings of the ACM on Computer Graphics and Interactive Techniques* 1, 1 (2018), 1–18.
- Min Tang, Dinesh Manocha, Jiang Lin, and Ruofeng Tong. 2011. Collision-streams: Fast GPU-based collision detection for deformable models. In *Symposium on interactive 3D graphics and games*. 63–70.
- Min Tang, Ruofeng Tong, Rahul Narain, Chang Meng, and Dinesh Manocha. 2013. A GPU-based streaming algorithm for high-resolution cloth simulation. In *Computer Graphics Forum*, Vol. 32. Wiley Online Library, 21–30.
- Min Tang, Tongtong Wang, Zhongyuan Liu, Ruofeng Tong, and Dinesh Manocha. 2018b. I-Cloth: Incremental collision handling for GPU-based interactive cloth simulation. *ACM Transactions on Graphics (TOG)* 37, 6 (2018), 1–10.



- Matthias Teschner, Stefan Kimmerle, Bruno Heidelberger, Gabriel Zachmann, Laks Raghupathi, Arnulph Fuhrmann, M-P Cani, François Faure, Nadia Magnenat-Thalmann, Wolfgang Strasser, et al. 2005. Collision detection for deformable objects. In *Computer graphics forum*, Vol. 24. Wiley Online Library, 61–81.
- Pascal Volino and Nadia Magnenat-Thalmann. 2006. Resolving surface collisions through intersection contour minimization. *ACM Transactions on Graphics (TOG)* 25, 3 (2006), 1154–1159.
- Huamin Wang. 2021. GPU-based simulation of cloth wrinkles at submillimeter levels. *ACM Transactions on Graphics (TOG)* 40, 4 (2021), 1–14.
- Jiahong Wang, Yinwei Du, Stelian Coros, and Thomaszewski. 2024. Neural Modes: Self-supervised Learning of Nonlinear Modal Subspaces. *IEEE/CVF Conf. on Computer Vision and Pattern Recognition (CVPR)*.
- Tongtong Wang, Zhihua Liu, Min Tang, Ruofeng Tong, and Dinesh Manocha. 2017. Efficient and Reliable Self-Collision Culling Using Unprojected Normal Cones. In *Computer Graphics Forum*, Vol. 36. Wiley Online Library, 487–498.
- Longhua Wu, Botao Wu, Yin Yang, and Huamin Wang. 2020. A safe and fast repulsion method for GPU-based cloth self collisions. *ACM Transactions on Graphics (TOG)* 40, 1 (2020), 1–18.
- Juntao Ye, Guanghui Ma, Liguang Jiang, Lan Chen, Jituo Li, Gang Xiong, Xiaoping Zhang, and Min Tang. 2017. A unified cloth untangling framework through discrete collision detection. In *Computer Graphics Forum*, Vol. 36. Wiley Online Library, 217–228.
- Juntao Ye, Timo R Nyberg, and Gang Xiong. 2015. Fast discrete intersection detection for cloth penetration resolution. In *2015 IEEE International Conference on Multimedia Big Data*. IEEE, 352–357.
- Juntao Ye and Jing Zhao. 2012. The intersection contour minimization method for untangling oriented deformable surfaces. In *Proceedings of the ACM SIGGRAPH/Eurographics Symposium on Computer Animation*. 311–316.
- Yueqi Zhong. 2009. Fast penetration resolving for multi-layered virtual garment dressing. *Textile Research Journal* 79, 9 (2009), 815–821.

## A INTERSECTION CONTOUR GRADIENT DERIVATION

As shown in Figure 4 of the paper, we decompose the gradient of the Intersection Contour Loss into two components. One component distorts the intersecting faces (green arrows), while another applies quasi-rigid translation.

Here we show the derivation for both of these components in a simple case where a triangle  $\triangle ABC$  penetrates an orthogonal plane with normal vector  $\vec{n}$ , as in Figure 4.

We derive the gradient of the loss function  $\mathcal{L}_{IC}$  with respect to the position of the node  $A$ . Thus we will only consider the penetration between the edge  $AB$  and the plane. The derivation for edge  $BC$  and other nodes follows the same steps.

Both edges of the triangle  $\triangle ABC$  penetrate the plane.  $AB$  penetrates it in the point  $p_{I_i}^0$ , while  $BC$  in the point  $p_{I_i}^1$ . We can compute the relative positions of the intersecting points  $s_0$  and  $s_1$  on each of these edges.

For  $s_0$ , we have

$$s_0 = \frac{(x_\Delta \cdot \vec{n}) - (A \cdot \vec{n})}{(B - A) \cdot \vec{n}}, \quad (13)$$

where  $x_\Delta$  is a point on the intersecting plane and  $\vec{n}$  is the plane’s normal. We compute the position of the intersection point and the loss value as

$$p_{I_i}^0 = A + s_0(B - A) \quad (14)$$

$$\mathcal{L}_{IC} = \|p_{I_i}^0 - p_{I_i}^1\|^2 \quad (15)$$

From Eq. 15 we can derive the gradient of  $\mathcal{L}_{IC}$  with respect to  $p_{I_i}^0$  as

$$\frac{\partial \mathcal{L}_{IC}}{\partial p_{I_i}^0} = 2(p_{I_i}^0 - p_{I_i}^1). \quad (16)$$

outfit name	garments	nodes	avg. fps
<i>cindy_020</i>	2	12030	10.49
<i>caren_008</i>	2	14003	10.18
<i>aaron_022</i>	3	17745	9.33
<i>celina_002</i>	3	20218	6.2
<i>ben_004</i>	5	36515	3.66

**Table 2: Number of garments and garment nodes in each of the five validation outfits from BEDLAM [Black et al. 2023]. We also list the average inference speed for each outfit. We run simulations with a time step of 1/30s. The timings were obtained using a single NVIDIA GeForce RTX 4090 GPU.**

The gradient of  $p_{I_i}^0$  w.r.t.  $A$  comprises a *distortional* and a *translational* component:

$$\frac{dp_{I_i}^0}{dA} = \frac{\partial p_{I_i}^0}{\partial A} + \frac{\partial p_{I_i}^0}{\partial s_0} \frac{\partial s_0}{\partial A} \quad (17)$$

For the *distortional* component, we have

$$\frac{\partial p_{I_i}^0}{\partial A} = (1 - s_0)I. \quad (18)$$

The *translational* component follows as

$$\frac{\partial p_{I_i}^0}{\partial s_0} = B - A \quad (19)$$

$$\frac{\partial s_0}{\partial A} = \frac{\vec{n} \cdot (x_\Delta - A)}{\vec{n} \cdot (B - A)} \vec{n} = k\vec{n}, \quad (20)$$

This is the derivative of  $s_0$  over  $A$  (see Eq. 13). For brevity, we substitute the scalar term in front of  $\vec{n}$  with  $k$ .

We can now write the full *translational* component as

$$\frac{\partial p_{I_i}^0}{\partial s_0} \frac{\partial s_0}{\partial A} = k(B - A)\vec{n}^T. \quad (21)$$

Finally, writing the full gradient of  $\mathcal{L}_{IC}$  with respect to  $A$ , we again identify two components,

$$\frac{d\mathcal{L}_{IC}}{dA} = \frac{d\mathcal{L}_{IC}}{dp_{I_i}^0} \frac{dp_{I_i}^0}{dA} \quad (22)$$

$$= \frac{d\mathcal{L}_{IC}}{dp_{I_i}^0} \frac{\partial p_{I_i}^0}{\partial A} + \frac{d\mathcal{L}_{IC}}{dp_{I_i}^0} \frac{\partial p_{I_i}^0}{\partial s_0} \frac{\partial s_0}{\partial A} \quad (23)$$

$$= 2(1 - s_0)(p_{I_i}^0 - p_{I_i}^1) + 2k((p_{I_i}^0 - p_{I_i}^1)^T(B - A))\vec{n}. \quad (24)$$

It is evident that the direction of the *distortional* component is  $p_{I_i}^0 - p_{I_i}^1$ , which is *parallel* to the intersecting plane. The direction of the *translational* component is  $\vec{n}$ , which is *orthogonal* to the intersecting plane. To supervise our model we only use the *translational* component.

## B EXPERIMENT DETAILS

### B.1 Validation outfits

For our experiments, we use 5 multi-garment outfits from BEDLAM [Black et al. 2023] dataset. We downsample some of them to have a smaller number of nodes and fit on a single GPU during inference.

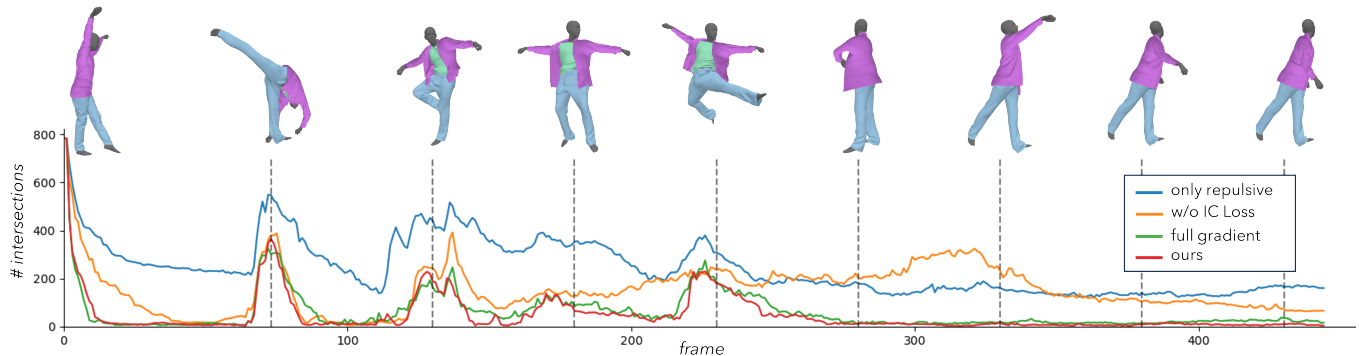


**Figure 6:** For one of the validation sequences, we plot the number of intersecting triangle pairs for all compared ablations. Starting from an intersecting geometry, our method quickly resolves most penetrations. During dynamic and complex motion sequences (for instance, those with body self-intersections), it may miss new penetrations but then is able to recover from them as well.

Table 2 shows the information on each outfit including the number of garments, total number of nodes, and average inference speed on validation sequences.

## B.2 Perceptual study

Here we provide a detailed description of the perceptual study presented in Section 5.3 of the main paper. We compare four methods: ContourCraft, HOOD [Grigorev et al. 2023], linear blend skinning (LBS), and the commercial software CLO3D [2022]. HOOD simulates garments without considering interactions between pieces of cloth, which results in many overlaps and intersections within and between garments. LBS rigidly attaches clothing to the nearest part of the body, which doesn’t capture the natural movement of loose clothing very well.

For the study, we simulated eight different pose sequences and body shapes, consistent across all methods. Each method produced eight videos of the simulations, all with the same camera settings.

In the first part of the study, the participants were shown individual simulation videos and asked to rate them from 1 to 5. The specific question asked was: “Mark how much do you agree with the following statement: «The motions of the clothing in the video are realistic and closely resemble how similar clothing would move in real life»”. The participants had to choose out of 5 options: “1 (completely disagree)”, “2 (disagree)”, “3 (neither agree nor disagree)”, “4 (agree)” or “5 (completely agree)”.

The order in which the videos were presented was randomized. Each video received ratings from 22 different participants. Given that there were 8 sequences for each method, each method was evaluated 176 times in total.

In the second part of our study, we performed a direct side-by-side comparison between three pairs of methods, where each pair included CLO3D and one of the other simulation methods. Participants were presented with two videos at a time—one from CLO3D and one from another method—and were asked to select which video demonstrates a more realistic simulation. The exact formulation was: *In this task, you will see two animations of a character in which the motion of the clothing is digitally simulated. Your task is to choose which clothing simulation is more realistic. Please pay*

*attention to the behavior of the clothing and not its colors. Ignore the way the body moves.* The sequence of the video pairs and the order of the videos within each pair were randomized. Each pair of videos was evaluated by 37 different participants, resulting in each method pair being compared 296 times in total

## C IMPLEMENTATION DETAILS

### C.1 Building input graph

The model’s input graph consists of the nodes of the outfit mesh  $V^G$ , nodes of the body mesh  $V^B$ , and several sets of edges.

We start by initializing the graph with nodes  $V^G$  and edges  $E^G$  of the garment. Then, we expand this by adding two levels of coarse edges  $E^{C_i}$  (with  $i$  indicating the level index). In the paper, these edges are included in  $E^G$  for simplicity. For a detailed explanation of how these edges are constructed, please see the Supplementary Material of HOOD [2023].

Next, we identify the nearest body node for each garment node. If they are closer than a threshold distance of  $\epsilon = 3cm$ , we create a body edge between them. Finally, we follow Algorithm 2 of the main paper to add two sets of ‘world edges’ between the garment nodes that are nearby in world coordinates. These edges are categorized as ‘repulsive’  $E_R^W$  and ‘non-repulsive’  $E_{NR}^W$ , based on their positions relative to intersection contours.

In the end, the input graph can be represented as:

$$G = \{V^G, E^G, V^B, E^B, E^{C_i}, E_R^W, E_{NR}^W\}$$

Each node and edge in this graph is assigned a feature vector that includes physical data and additional parameters. We normalize these feature vectors to ensure that the distribution of each parameter approximates a normal distribution  $\mathcal{N}(0, I)$ . This helps the model to converge. For more information on this process, refer to MeshGraphNets [2020].

### C.2 Network architecture

Our model follows the architecture used in HOOD [2023], which includes an encoder, 15 message-passing steps, and a decoder. Each component consists of multiple multi-layer perceptrons (MLPs)

with 2 hidden layers each and a latent dimension of 128. We use ReLU activation functions and layer normalization for these hidden layers, but no activation function in the output layer.

The **encoder** processes the input feature vectors of all nodes and edges to map them into a latent space. Each type of edge and the nodes have their dedicated MLP. These encoder MLPs output vectors of dimension 128, with the input dimension corresponding to the number of parameters each node or edge has.

Each **message-passing** step also contains MLPs for each edge set and an MLP for nodes. It first updates the latent vectors of each edge. This is done by concatenating the latent vector of each edge with the latent vectors of the nodes it connects to, and then feeding this combined vector into the corresponding MLP. The input dimension for these edge-specific MLPs is  $128 \times 3$ , and they output vectors of dimension 128. Next, the step updates nodal latent vectors. This involves first aggregating the latent vectors from all the edges connected to a node, done separately for each set of edges. These aggregated vectors, along with the latent vector of the node itself, are then concatenated and processed through another MLP to generate the updated nodal vector. The input dimension for these nodal MLPs is  $128 \times 6$ , where 6 is the number of edge sets and an output dimension of 128.

For more details on the message-passing process please refer to MeshGraphNets [2020] and the Supp. Mat. of HOOD [2023].

Finally, the **decoder** uses its MLP to transform the latent vectors of the garment nodes, each of size 128, into nodal acceleration vectors of size 3. These acceleration vectors are subsequently de-normalized using pseudo-statistics derived from sequences generated by linear blend skinning. For more detailed information on this process, please refer to MeshGraphNets [2020] and the Supp. Mat. of HOOD [2023].

### C.3 Autoregressive training

Following HOOD, we gradually increase the number of autoregressive steps in each training sample from 1 to 5 every 5000 iterations. In the second and third stages, we also include full-length pose sequences of up to 150 frames each. In these stages, we also alternate between training samples with and without cloth–cloth interactions. For that, in every second training iteration, we omit cloth–cloth correspondences and the respective objective terms, falling back to the process from the first stage. This helps the model avoid diverging from generating realistic collision-agnostic behavior of the fabric.